

Walking with Confidence: Safety Regulation for Full Order Biped Models

Nils Smit-Anseeuw, C. David Remy, and Ram Vasudevan

Abstract—Safety guarantees are valuable in the control of walking robots, as falling can be both dangerous and costly. Unfortunately, set-based tools for generating safety guarantees (such as sums-of-squares optimization) are typically restricted to simplified, low-dimensional models of walking robots. For more complex models, methods based on hybrid zero dynamics can ensure the local stability of a pre-specified limit cycle, but provide limited guarantees. This paper combines the benefits of both approaches by using sums-of-squares optimization on a hybrid zero dynamics manifold to generate a guaranteed safe set for a 10-dimensional walking robot model. Along with this set, this paper describes how to generate a controller that maintains safety by modifying the manifold parameters when on the edge of the safe set. The proposed approach, which is applied to a bipedal Rabbit model, provides a roadmap for applying sums-of-squares verification techniques to high dimensional systems. This opens the door for a broad set of tools that can generate safety guarantees and regulating controllers for complex walking robot models.

I. INTRODUCTION

Avoiding falls is a safety critical and challenging task for legged robotic systems. This challenge is compounded by strong limits on the available actuation torques; particularly at the ankle or ground contact point. These limits in actuation mean that the motion of a legged robot is often dominated by its mechanical dynamics, which are hybrid, nonlinear, and unstable. A consequence of these limitations is that a controller might be required to take a safety preserving action well before the moment a failure occurs.

Consider, for example, a bipedal robot that just entered single stance during a fast walking gait. The robot is pivoting dynamically over the stance foot and can only apply limited ankle torques to control its motion. To catch the robot again, the swing foot needs to be brought forward rapidly and be placed well in front of the robot. If the forward velocity of the robot and hence the pivoting motion is too fast, there will not be enough time to complete this foot placement far enough in front of the stance leg to slow the robot down [1]. As a result, the robot's speed increases further, leaving even less time for leg swing in the subsequent steps. The robot might manage to complete another couple of strides, but at this point a fall is inevitable and no control action can prevent it.

Knowing the limits of safe operation is akin to knowing the set of states from which falls, even in the distant future, can be avoided. Such knowledge is valuable for many reasons. Knowing that a fall is inevitable is useful in itself, as it allows a robot to brace for the imminent impact. Knowing the distance from the border of the safe set could allow a robot to estimate the set of impulses that can be withstood without failing. This would allow it to judge whether or not it can

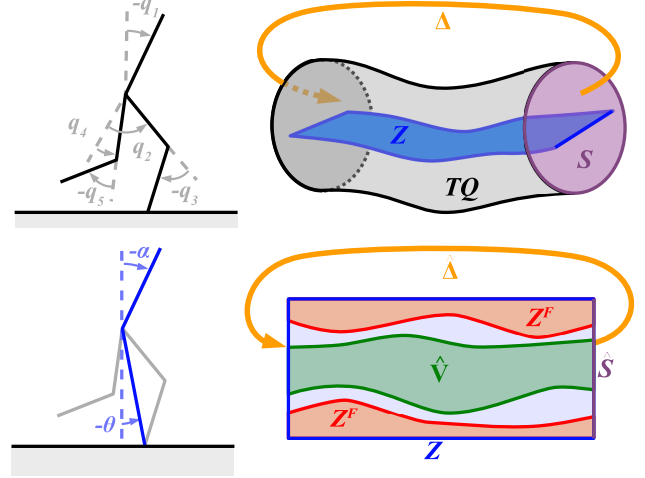


Fig. 1. Generating safety guarantees for a high dimensional robot (illustrated on Rabbit [3]). The state-space of the full robot is given in the top right figure, where TQ is the tangent space on Q , S is the hybrid guard representing foot touchdown, and Δ is the corresponding discrete reset map. Using feedback linearization, we restrict our states to lie on a low-dimensional manifold Z , reducing the state-space dimension to an amenable size for sums-of-squares analysis. This manifold is parameterized by a set of states that are important for safety (e.g. for Rabbit we chose the pitch angle α and stance leg angle θ). The shaping parameters α can be modified in real-time by a control input, allowing for safety regulating behaviours on Z . To guarantee safety on Z we find the set of unsafe states Z^F from which the state may leave the manifold (for instance due to motor torque limits). We then use sums-of-squares tools [4] to find a control invariant set $\hat{V} \subset Z \setminus Z^F$. This control invariant set can be used to define a semi-autonomous, guaranteed safe controller for the full robot dynamics.

safely interact with the environment in a given situation; for example, to push a cart while walking. In terms of control, the value lies in the flexibility this knowledge can create. Rather than stabilizing the robot motion along a specified trajectory, one could imagine controllers that are adaptive to adjust to the environment, to maximize performance, or to fulfill a secondary task such as pointing a sensor onto a target. All these secondary goals can be pursued as long as the state of the robot is within the safe set.

In this context, a representation of the set of safe states enables the construction of a regulator that monitors the system state and takes safety preserving actions only when the robot is at risk of failure [2]. Such a regulator could guarantee safe operation, while allowing a secondary control system to behave flexibly as long as safety is not threatened.

Identifying such safety limits, however, is a challenging problem for nonlinear and hybrid systems. A promising tool for identifying the safety limits of a legged robotic system is sums-of-squares (SoS) optimization [4]. This approach uses semi-definite programming to identify the limits of safety in the state space of a system as well as associated controllers for a broad class of nonlinear [5], [6], [7] and

hybrid systems [8], [9], [10]. These safe sets can take the form of *reachable sets* (sets that can reach a known safe state) [11], [9], [5] or *invariant sets* (sets whose members can be controlled to remain in the set indefinitely) in state space [12], [8], [13]. However, the representation of each of these sets in state space severely restricts the size of the problem that can be tackled by these approaches. To accommodate this limitation, sums-of-squares analysis has been primarily applied to reduced models of walking robots: ranging from spring mass models [14], to inverted pendulum models [11], [15] and to inverted pendulum models with an offset torso mass [13]. The substantial differences between these simple models and real robots causes difficulty when applying these results to hardware.

A contrasting approach to designing stable controllers for high dimensional, underactuated robot models uses hybrid zero dynamics (HZD) [16]. In this approach, feedback linearization is used to drive the actuated degrees of freedom of the robot towards a lower dimensional hybrid zero dynamics manifold. This manifold is specified as the zero levelset of a configuration-dependent output vector and represents the motion of the robot in its underactuated degrees of freedom.

Current approaches for guaranteeing safe HZD control [17], [18], [19], [20], [21] all rely on the Poincaré stability of a periodic limit cycle. In many of these approaches, safety is contingent on the feasibility of a real-time Quadratic Program (QP) [18], [19], [20], [21] that is dependent on the underactuated coordinates of the system. Guaranteeing feasibility of this QP thus requires a bound on these degrees of freedom. So far, such a bound has relied on local limit-cycle stability, which precludes recovery behaviors that would leave the neighborhood of the limit cycle. To overcome this drawback, some methods combine a family of periodic gaits into a gait-library [22], [23]. The gait-library approach can use non-local recovery behaviour to demonstrate impressive robustness, however finding the limits of safety remains an open challenge.

This paper builds on these two broad approaches to safety and control synthesis for legged robotic systems. To combine the full-model accuracy of hybrid zero dynamics and the set-based safety guarantees of sums-of-squares programming, we propose the following approach (Fig. 1). First, we use hybrid zero dynamics to map the full order dynamics to a low dimensional hybrid manifold. We control the dynamics on the manifold using a set of *shaping parameters*, which are modified in continuous time to regulate safety. We then use sums-of-squares programming to find a subset of this manifold which can be rendered forward control invariant. Once this subset is found on the low dimensional manifold, a regulator can be constructed that allows for free control of the manifold dynamics when safety is not at risk, but switches to a safety preserving controller when safety is threatened.

The approach is presented in a general form that extends to a large class of underactuated bipedal robots. Throughout the paper, an example implementation is given for a 10-dimensional model of the robot Rabbit [3] and a tracking task is used to illustrate semi-autonomous safe control. To

the best of our knowledge, this is the highest dimensional walking robot model for which set-based safety guarantees have been generated thus far.

The rest of this paper is organized as follows: Section II formally defines the assumptions and objective of this paper. The next two sections describe our method. Section III constructs a low dimensional zero dynamics manifold with control input. In Section IV we present a sums-of-squares optimization which finds a control invariant subset of the manifold that avoids a designated set of unsafe states. Section V describes the results of our implementation on the robot Rabbit [3], and conclusions are presented in Section VI.

II. PROBLEM SETUP

A. Robot Model

For simplicity, we apply similar modeling assumptions to those made in [16]. We begin by assuming robot hypotheses RH1-6 formally stated in [16]. That is, the robot is modeled as a planar chain of rigid links with mass. Each joint is directly torque actuated except for the point of contact with the ground, leading to one degree of underactuation for a planar model. Next, we impose the gait hypotheses GH1-4 and GH6 in [16] as conditions for a walking gait. That is, the robot must walk continuously forward in alternating phases of single support and (instantaneous) double support. We do not require the gait to be left-right symmetric (i.e. GH5).

The full configuration of the robot is given by the set of joint angles $q = \{q_1, \dots, q_{n_q}\} \in Q \subset \mathbb{R}^{n_q}$. We next define the set of *feasible* configurations $\tilde{Q} \subset Q$:

Definition 1. A configuration is feasible if the joint angles satisfy actuator limits, and only foot points are touching the ground (i.e. the robot has not fallen over).

Using the method of Lagrange, we can obtain a continuous dynamic model of the robot during swing phase:

$$\dot{x}(t) = f(x(t)) + g(x(t))u(t). \quad (1)$$

where $x(t) = [q^\top(t), \dot{q}^\top(t)]^\top \in TQ \subset \mathbb{R}^{2n_q}$ denotes the tangent space of Q , $u(t) \in U$, U describes the permitted inputs to the system, and t denotes time.

We assume that an impact event happens for each stride, following the impact hypotheses IH1-6 in [16]. That is an impact is assumed to be instantaneous and impulsive, with the stance leg leaving the ground immediately after impact. Using a similar approach to [16], we can construct a reset map for the state after impact:

$$x(t^+) := \Delta(x(t^-)) \quad (2)$$

$$= \begin{bmatrix} \Delta_q q(t^-) \\ \Delta_{\dot{q}}(q(t^-)) \dot{q}(t^-) \end{bmatrix}. \quad (3)$$

Here the superscript plus indicates the time just after the event and the superscript minus indicates the time just before the event. $\Delta : TQ \rightarrow TQ$ is the reset map of the robot state. $\Delta_q \in \mathbb{R}^{n_q \times n_q}$ is a coordinate transformation matrix that swaps the swing leg and the stance leg after impact. $\Delta_{\dot{q}} : Q \rightarrow \mathbb{R}^{n_q \times n_q}$, is the configuration-dependent reset map of the configuration velocities.

This equation holds true for all states in $S \subset TQ$, which is called the *guard* of the hybrid system, and represents the states of the robot with zero swing foot height and downwards swing foot velocity. Any time the state of the robot enters S , the reset event must occur.

Example 1. The configuration q for Rabbit is shown in Figure 1 (top left). \tilde{Q} is the set of robot configurations in which only foot points intersect the ground and all joints are within the limits: $q_1, q_2, q_4 \in [-\pi/2, \pi/2]$, $q_3, q_5 \in [-\pi/2, 0]$. When the swing foot intersects with the ground, we enter the guard S . This causes an impulse to be transmitted to the colliding foot, and the swing and stance feet swap. The impulse and coordinate swap are given by Δ . The input torques can take values in the interval $U = [-30 \text{ Nm}, 30 \text{ Nm}]^4$.

B. Safety

In this paper, *safety* is defined as keeping the configuration *feasible* for all time (i.e. $q(t) \in \tilde{Q}, \forall t$). To guarantee safety, this paper finds a *Viability Domain* [12]:

Definition 2. A Viability Domain $V \subset \mathbb{R}^{2n_q}$ is any set satisfying $V \subset T\tilde{Q}$ which is also forward control invariant. That is, there exists a Lipschitz state feedback controller $u_s : T\tilde{Q} \rightarrow U$, such that for every initial condition $x_0 \in V$, the execution of the system from the initial condition remains in V for all time $t \in [0, \infty)$. We refer to any feedback controller that is able to ensure that the system is forward control invariant as an Autonomous Viable Controller.

The forward control invariance property ensures that any state that begins within a viability domain V can be controlled to remain within the domain. Since V contains only feasible configurations ($V \subset T\tilde{Q}$), we know that safety can be maintained by at least one controller from all states in V .

Once a viability domain is found, we use it to construct a semi-autonomous, safety preserving controller. Given an initial state within V , a user defined control input is applied without modification to the system. The state of the system is then continuously monitored. If the state approaches the boundary of the viability domain, the control input is overridden by an autonomous viable controller. This gives the user full control over the system until safety is threatened, at which point, safety is automatically enforced. Once safety is no longer at risk, control is returned to the user.

C. Goal

Using these definitions, we state our objective as:

- 1) Find a viability domain and a corresponding autonomous viable controller.
- 2) Use this domain and autonomous viable controller to construct a semi-autonomous viable controller.

III. CONTROLLED HYBRID ZERO DYNAMICS MANIFOLD

We intend to use sums-of-squares optimization to achieve these objectives. However, the state-space dimension of realistic robot models far exceeds the limits of this tool. For instance, the state-space of the benchmark model Rabbit [3]

has dimension 10, while many sums-of-squares problems become computationally challenging above dimension 6 [13]. In this section, we show how the the state-space dimension can be reduced to a feasible size using the idea of hybrid zero dynamics [16].

A. Shaping Parameters

The hybrid zero dynamics approach uses feedback linearization to drive the actuated degrees of freedom onto a low-dimensional manifold specified by a set of user-chosen outputs, which depend on the robot configuration $q \in Q$. We modify this approach by making these outputs additionally depend on a set of time varying shaping parameters $\alpha(t) \in A \subset \mathbb{R}^{n_\alpha}$. The shaping parameters α are used in this paper to provide an input within the manifold dynamics. By varying α continuously over time, the user can change the dynamics of the hybrid zero dynamics manifold to control the robot. The idea of modifying HZD manifold parameters to improve stability is similar to prior work [24], where parameters are allowed to change discretely once per robot step. In contrast, we allow α to vary throughout the step, enabling a rapid response to disturbance without waiting for the next discrete update.

We define the dynamics of α as:

$$\dot{x}_\alpha(t) = f_\alpha(x_\alpha(t)) + g_\alpha(x_\alpha(t))u_\alpha(t), \quad (4)$$

where $x_\alpha(t) = [\alpha^\top(t), \dot{\alpha}^\top(t)]^\top \in TA$, $u_\alpha(t) \in U_\alpha \subset \mathbb{R}^{n_\alpha}$ are the shaping parameter inputs (with permitted values U_α), and t denotes time. We require that α has vector relative degree two under these dynamics. We assume a trivial discrete update for the shaping parameters when the robot state hits a guard: $x_\alpha(t^+) = x_\alpha(t^-)$.

Example 2. As shown in the bottom left of Figure 1, we use a single shaping parameter $\alpha(t) \in [-\pi/2, \pi/2]$ to modify the desired pitch angle of Rabbit. This choice of shaping parameter is motivated by the observation that torso lean is an effective speed regulator for underactuated bipeds [25]. We define the dynamics of α as follows:

$$\frac{d}{dt} \begin{bmatrix} \alpha(t) \\ \dot{\alpha}(t) \end{bmatrix} = \begin{bmatrix} \dot{\alpha}(t) \\ 0 \end{bmatrix} + \begin{bmatrix} 0 \\ 1 \end{bmatrix} u_\alpha(t), \quad (5)$$

where u_α represents the user-controlled pitch acceleration.

B. Continuous Zero Dynamics

This subsection constructs the continuous portion of our controlled hybrid zero dynamics. We begin by defining a set of outputs h , which implicitly specify points on the manifold. Next we define a function θ which maps from points in the state space to points in the manifold and gives us a parametrization of our manifold states. We then define a feedback controller u^* which renders the manifold invariant, allowing us to obtain continuous manifold dynamics.

Throughout the section, we use \mathcal{L}_f^x and \mathcal{L}_g^x to represent the Lie derivatives in TQ with respect to f and g , and $\mathcal{L}_{f_\alpha}^{x_\alpha}$ and $\mathcal{L}_{g_\alpha}^{x_\alpha}$ to represent the Lie derivatives in TA with respect to f_α and g_α (where we dropped all of the arguments). We define the manifold implicitly as the zero level-set of a set

of outputs: $h : Q \times A \rightarrow \mathbb{R}^{n_u}$, which are required to satisfy the following hypotheses (modified from [16]).

HH 1. h is a function of only the configuration variables and the shaping parameters;

HH 2. for each point $(q, \alpha) \in Q \times A$, the decoupling matrix $(\mathcal{L}_g^x(\mathcal{L}_f^x h + \mathcal{L}_{f_\alpha}^{x_\alpha} h))(q, \alpha)$ is square and invertible;

HH 3. there exists a smooth function $\theta : Q \rightarrow \mathbb{R}^{n_q - n_u}$ such that the map $\Phi : Q \times A \rightarrow \mathbb{R}^{n_q + n_\alpha}$ given by $\Phi(q, \alpha) := [h(q, \alpha), \theta(q), \alpha]^\top$ is a diffeomorphism onto its image, and

HH 4. $h(q, \alpha) = 0$ for at least one point $(q, \alpha) \in Q \times A$.

These hypotheses allow us to construct a continuous zero dynamics manifold Z and associated controller u^* :

Theorem 1. $Z := \{(q, \alpha, \dot{q}, \dot{\alpha}) \in TQ \times TA \mid h(q, \alpha) = 0, (\mathcal{L}_f^x h)(q, \alpha, \dot{q}) + (\mathcal{L}_{f_\alpha}^{x_\alpha} h)(q, \alpha, \dot{\alpha}) = 0\}$ is a smooth sub-manifold in $TQ \times TA$ of dimension $n_z = 2(n_q - n_u + n_\alpha)$. The control input $u^* : TQ \times TA \times U_\alpha \rightarrow U$ given by:

$$u^*(x, x_\alpha, u_\alpha) = -(\mathcal{L}_g^x(\mathcal{L}_f^x h + \mathcal{L}_{f_\alpha}^{x_\alpha} h))^{-1} \left(\mathcal{L}_f^x(\mathcal{L}_f^x h + \mathcal{L}_{f_\alpha}^{x_\alpha} h) + \mathcal{L}_{g_\alpha}^{x_\alpha}(\mathcal{L}_f^x h + \mathcal{L}_{f_\alpha}^{x_\alpha} h)u_\alpha + \mathcal{L}_{f_\alpha}^{x_\alpha}(\mathcal{L}_f^x h + \mathcal{L}_{f_\alpha}^{x_\alpha} h) \right) \quad (6)$$

renders Z invariant under the continuous dynamics (note the right hand side arguments are suppressed to simplify presentation).

The proof of this theorem follows immediately from the hypotheses using results in [26, Chapter 9.3.2].

The diffeomorphism in HH3 implies a parameterization of the on-manifold states $\hat{x}(t) \in Z$ as: $\hat{x}(t) = [\theta(q)^\top, \dot{\theta}(q, \dot{q})^\top, \alpha^\top, \dot{\alpha}^\top]^\top$ (where we have suppressed the time dependence on the right hand side). The continuous dynamics under this parameterization are then:

$$\dot{\hat{x}} = \begin{bmatrix} \dot{\theta} \\ \mathcal{L}_f^x \mathcal{L}_f^x \theta + \mathcal{L}_g^x \mathcal{L}_f^x \theta u^* \\ f_\alpha + g_\alpha u_\alpha \end{bmatrix} = \hat{f}(\hat{x}) + \hat{g}(\hat{x})u_\alpha, \quad (7)$$

where we have suppressed the time dependence. It is helpful to define the coordinate transform from the manifold parameters to the ambient space $q_0 : Z \rightarrow Q$ as:

$$\begin{bmatrix} q_0(\theta, \alpha) \\ \alpha \end{bmatrix} := \Phi^{-1} \begin{bmatrix} [0, \dots, 0]^\top \\ \theta \\ \alpha \end{bmatrix}, \quad (8)$$

i.e. $q_0(\theta, \alpha)$ is the configuration of the point $(\theta, \dot{\theta}, \alpha, \dot{\alpha}) \in Z$.

Example 3. We begin by using the trajectory optimization toolbox FROST [27] to find a time-varying, periodic walking trajectory: $q^F : [0, t_{max}] \rightarrow Q$. For this trajectory, the stance leg angle of the robot: $\theta(q) = -q_1 - q_2 - \frac{q_3}{2}$ is monotonic in time and varies from θ_{min} to θ_{max} . This allows us to define a phasing function $t_\theta : [\theta_{min}, \theta_{max}] \rightarrow [0, t_{max}]$ which satisfies $q^F(t_\theta(\theta(q^F(t)))) = q^F(t)$ (i.e. t_θ maps from points in the state space to points along the trajectory).

We modify the pitch angle of the FROST trajectory using the shaping parameter α , giving us the output function:

$$h(q, \alpha) = \begin{bmatrix} q_1 - q_1^F(t_\theta(\theta(q))) - \alpha \\ q_3 - q_3^F(t_\theta(\theta(q))) \\ q_4 - q_4^F(t_\theta(\theta(q))) + \alpha \\ q_5 - q_5^F(t_\theta(\theta(q))) \end{bmatrix} + h_m(\theta(q), \alpha). \quad (9)$$

Here we also added the function $h_m : Q \times A \rightarrow \mathbb{R}^4$ which ensures the satisfaction of the hybrid invariance condition (discussed in the next section).

C. Hybrid Zero Dynamics

For the zero dynamics manifold to be forward invariant for the hybrid system, it must map onto itself through the guard and reset. This gives us the *hybrid invariance condition*, which states that the zero dynamics manifold Z must satisfy:

$$\begin{bmatrix} \Delta(x(t^-)) \\ x_\alpha(t^-) \end{bmatrix} \in Z \quad (10)$$

for all $[x(t^-), x_\alpha(t^-)]^\top \in Z \cap (S \times A)$.

Using the definition of Z , this can be re-stated as:

$$h(q(t^+), \alpha(t^-)) = 0 \quad (11)$$

$$\begin{aligned} \mathcal{L}_f^x h(q(t^+), \dot{q}(t^+), \alpha(t^-)) + \\ + \mathcal{L}_{f_\alpha}^{x_\alpha} h(q(t^+), \alpha(t^-), \dot{\alpha}(t^-)) = 0 \end{aligned} \quad (12)$$

for all $[x(t^-), x_\alpha(t^-)]^\top \in Z \cap (S \times A)$, where $[q(t^+), \dot{q}(t^+)]^\top = \Delta(x(t^-))$.

If these conditions are satisfied, we call Z a *hybrid zero dynamics manifold*, with dynamics given by:

$$\dot{\hat{x}}(t) = \hat{f}(\hat{x}(t)) + \hat{g}(\hat{x}(t))u_\alpha, \quad \forall \hat{x}(t) \notin \hat{S} \quad (13)$$

$$\hat{x}(t^+) = \hat{\Delta}(\hat{x}(t^-)), \quad \forall \hat{x}(t^-) \in \hat{S}. \quad (14)$$

\hat{S} and $\hat{\Delta}$ are the manifold guard and reset, respectively, defined as:

$$\hat{S} = \left\{ \hat{x} \in Z \mid \begin{bmatrix} q_0(\hat{x}) \\ \frac{dq_0}{dt}(\hat{x}) \end{bmatrix} \in S \right\} \quad (15)$$

$$\hat{\Delta}(\hat{x}(t^-)) = \begin{bmatrix} \theta(q(t^+)) \\ \frac{\partial \theta}{\partial q}(q(t^+))\dot{q}(t^+) \\ x_\alpha(t^-) \end{bmatrix}. \quad (16)$$

Example 4. For periodic q^F , (11) holds if $h_m(\theta_{min}, \alpha) = h_m(\theta_{max}, \alpha) = 0$. We follow a similar procedure to [16] to ensure that (12) is satisfied. This procedure gives:

$$h_m(\theta, \alpha) = m(\alpha)p_m(\theta) \quad (17)$$

Where $p_m : [\theta_{min}, \theta_{max}] \rightarrow \mathbb{R}$ is a cubic spline satisfying: $p_m(\theta_{min}) = p_m(\theta_{max}) = \frac{dp_m}{d\theta}(\theta_{max}) = 0$, $\frac{dp_m}{d\theta}(\theta_{min}) = 1$ and $m : A \rightarrow \mathbb{R}^4$ is given by:

$$m(\alpha) = -\frac{\frac{\partial h}{\partial q}^+ \Delta \dot{q}(q_0^-) \frac{\partial q_0^-}{\partial \theta}}{\frac{\partial \theta}{\partial q}^+ \Delta \dot{q}(q_0^-) \frac{\partial q_0^-}{\partial \theta}}, \quad (18)$$

where $\frac{\partial h}{\partial q}^+ = \frac{\partial h}{\partial q}(\theta_{min}, \alpha)$, $\frac{\partial \theta}{\partial q}^+ = \frac{\partial \theta}{\partial q}(\theta_{min}, \alpha)$, $q_0^- = q_0(\theta_{max}, \alpha)$ and $\frac{\partial q_0^-}{\partial \theta} = \frac{\partial q_0}{\partial \theta}(\theta_{max}, \alpha)$. The guard of our HZD manifold Z is given as $\hat{S} = \{\hat{x} \mid \theta = \theta_{max}, \dot{\theta} > 0\}$ and the reset is defined as in (16).

D. Safety on the Manifold

We now revisit the safety criteria from Section II-B under the assumption that our state is controlled to lie on Z . For the biped to be safe, we require that the manifold state remains in the feasible set \tilde{Q} , and that the state does not leave the manifold (either by leaving the manifold boundary, or by encountering actuator limits when trying to stay on Z). We define the *unsafe states* $Z^F \subset Z$ as the union of:

- The *infeasible* states: $((TQ \setminus T\tilde{Q}) \times TA) \cap Z$
- The states that *leave the manifold boundary*, i.e. all members of the boundary set $(\partial Z = \{\hat{x} \in Z \mid q_0(\hat{x}) \in \partial Q \text{ or } \alpha \in \partial A\})$ which do not lie on a guard, and that have an outward velocity.
- The states *requiring unattainable actuation* to remain on Z , i.e. all states $(x, x_\alpha) \in Z$ for which $u^*(x, x_\alpha, u_\alpha) \notin U, \forall u_\alpha \in U_\alpha$.

Additionally we define the state-dependent set of realizable shaping parameter inputs $\hat{U} : TQ \times TA \rightarrow 2^{U_\alpha}$, as $\hat{U}(x, x_\alpha) = \{u_\alpha \in U_\alpha \mid u^*(x, x_\alpha, u_\alpha) \in U\}$ (where 2^{U_α} denotes the set of all subsets of U_α).

Provided we constrain the manifold state to avoid Z^F , and constrain the shaping parameter input to lie within \hat{U} , our safety criteria is maintained.

Our goal from Section II-C can now be re-stated as:

- 1) Find a viability domain on Z that does not intersect Z^F , and an autonomous viable controller $\hat{u}_s : Z \rightarrow \hat{U}$.
- 2) Use this domain and autonomous viable controller to construct a semi-autonomous controller.

Example 5. For the Rabbit example, the set of states that leave the manifold boundary are given by $Z_{LMB} = \{\hat{x} \mid \alpha = \pi/2, \dot{\alpha} > 0\} \cup \{\hat{x} \mid \alpha = -\pi/2, \dot{\alpha} < 0\}$. All other states on the manifold boundary either lie on a guard ($\theta = \theta_{max}, \dot{\theta} > 0$), or flow inwards. We use sampling and fitting to find a region $Z_{Lim} \subset Z$ where the actuator torque limits can be satisfied for some u_α . We then define our unsafe set (see Fig. 2):

$$Z^F = (((TQ \setminus T\tilde{Q}) \times TA) \cap Z) \cup Z_{LMB} \cup (Z \setminus Z_{Lim}). \quad (19)$$

The set of attainable inputs \hat{U} is given by the minimum and maximum values of u_α at each sample point $(x, x_\alpha) \in Z$ that satisfy $u^*(x, x_\alpha, u_\alpha) \in U$.

IV. HYBRID CONTROL INVARIANT SET

This section outlines how the low dimensional safety problem from Section III-D can be solved using sums-of-squares optimization [4], [28]. Broadly, the sums-of-squares approach enforces constraints of the form $p \geq 0$ (where p is a function) by constraining p to be a sum-of-squares polynomial, i.e. $p = \sum_i p_i^2$ (where p_i are polynomials). We refer to this constraint as $p \in SoS$.

We begin by showing how the sets and dynamics from the preceding section can be represented using polynomials. We next define a bilinear semi-definite program for finding a viability domain, and describe the alternation used to solve it. Finally, we construct a guaranteed safe semi-autonomous

controller for the full robot, based on the resulting viability domain.

A. Polynomial Representation

For the dynamics of the system to be used inside our sums-of-squares program, they must be represented in a polynomial form. In particular, we require polynomial representations of the functions $\hat{f}, \hat{g}, \hat{\Delta}$ and the sets \hat{S}, Z^F, \hat{U} . Since these sets and functions can contain trigonometric as well as rational terms in their definition, we rely on approximate representations. It is important to take care to ensure that the safety guarantee is preserved under approximation.

We begin by sampling $\hat{f} : Z \rightarrow \mathbb{R}^{n_z}$ and $\hat{g} : Z \rightarrow \mathbb{R}^{n_z \times n_\alpha}$ over a grid of points in Z . Least-squares fitting can then be used to obtain the corresponding polynomial representations: \hat{f}_p and \hat{g}_p . To account for the approximation error in the continuous dynamics functions, we introduce a set of error-bounding polynomials $\hat{e}_p : Z \rightarrow \mathbb{R}^{n_z}$ which satisfy:

$$\hat{e}_p(\hat{x}) \geq \left| \hat{f}(\hat{x}) - \hat{f}_p(\hat{x}) + (\hat{g}(\hat{x}) - \hat{g}_p(\hat{x})) \hat{u} \right|, \quad (20)$$

for all $\hat{x} \in Z$ and $\hat{u} \in \hat{U}$ where the inequality and absolute value are taken element-wise. These polynomials can be found using a linear program that minimizes the integral of \hat{e}_p subject to (20) enforced at a set of sample points.

To represent sets in polynomial form, we require them to take the form of semi-algebraic sets (i.e. a set $X \subset Y$ is defined as $X = \{y \in Y \mid h_i(y) \geq 0, \forall i = 1, \dots, n\}$, where $h : Y \rightarrow \mathbb{R}^n$ is a collection of polynomials). We use a bounding set to approximate the reset map $\hat{\Delta} : \hat{S} \rightarrow Z$ in a conservative manner. That is, we find a set $R_p \subset Z \times Z$ that bounds all possible reset behaviours:

$$(\hat{x}, \hat{\Delta}(\hat{x})) \in R_p, \forall \hat{x} \in \hat{S}. \quad (21)$$

The sets \hat{S} and Z^F are represented with semi-algebraic outer approximations as follows: $Z_p^F \supset Z^F$, $\hat{S}_p \supset \hat{S}$. We define the sets R_p, Z_p^F, \hat{S}_p using the respective polynomials: $h_R : Z \times Z \rightarrow \mathbb{R}^{n_{hr}}$, $h_F : Z \rightarrow \mathbb{R}^{n_{hf}}$, $h_S : Z \rightarrow \mathbb{R}^{n_{hs}}$. The space of feasible inputs \hat{U} can be approximated using a state-dependent box constraint:

$$\hat{u}_{min}(\hat{x}) \leq \hat{u}(\hat{x}) \leq \hat{u}_{max}(\hat{x}), \forall \hat{x} \in Z \setminus Z_p^F \quad (22)$$

where $\hat{u}_{min}, \hat{u}_{max} : Z \setminus Z_p^F \rightarrow U_\alpha$ are polynomial input bounds, and the inequality is taken element-wise. The set of inputs that satisfy this box constraint is denoted by \hat{U}_p .

B. Optimization Formulation

We use an optimization similar to [13] to find the largest possible viability domain $\hat{V} \subset Z \setminus Z^F$ for our hybrid zero dynamics system. We represent \hat{V} as the zero super-levelset of a polynomial function $\hat{v} : Z \rightarrow \mathbb{R}$ (i.e. $\hat{V} = \{\hat{x} \in Z \mid \hat{v}(\hat{x}) \geq 0\}$), and represent the autonomous viable controller using a polynomial function $\hat{u}_s : Z \rightarrow \mathbb{R}^{n_\alpha}$. To enforce the viability of \hat{V} according to Definition 2, we require \hat{v} and \hat{u}_s to satisfy four conditions:

Viability Conditions.

- 1) \hat{V} does not intersect Z^F (i.e. $\hat{v}(\hat{x}) < 0, \forall \hat{x} \in Z^F$)

- 2) All states that are contained in both the guard and \hat{V} must be mapped to a state in \hat{V} (i.e. $\hat{v}(\hat{\Delta}(\hat{x})) \geq 0, \forall \hat{x} \in \{\hat{x} \in \hat{S} \mid \hat{v}(\hat{x}) \geq 0\}$)
- 3) At the boundary of \hat{V} (i.e. where $\hat{v}(\hat{x}) = 0$), the state flows inward under the controller \hat{u}_s (i.e. $\frac{d\hat{v}}{dt} > 0$)
- 4) The autonomous safe controller must satisfy the input bounds within the safe set (i.e. $\hat{u}_s(\hat{x}) \in \hat{U}, \forall \hat{x} \in \hat{V}$)

Condition 1 ensures that states can not leave the viability domain by simply leaving the space Z . Condition 2 ensures that states can not leave the viability domain when traversing a guard. Condition 3 ensures that states cannot leave the viability domain under the continuous dynamics of the system. Finally, Condition 4 ensures that our controller respects the robot torque constraints. Each of these conditions are ensured with a corresponding sums-of-squares constraint, giving us:

SoS Constraint 1. (Viability Condition 1)

$$-\hat{v} - \sigma_1 h_F \in SoS$$

Here $\sigma_1 : Z \rightarrow \mathbb{R}^{1 \times n_{hf}} \in SoS$ are s-functions [4] that relax the positivity constraint outside Z_p^F .

SoS Constraint 2. (Viability Condition 2)

$$\hat{v}^+ - \hat{v}^- - \sigma_2 h_R - \sigma_3 h_S^- \in SoS$$

Here $\sigma_2 : Z \times Z \rightarrow \mathbb{R}^{1 \times n_{hr}}, \sigma_3 : Z \rightarrow \mathbb{R}^{1 \times n_{hs}} \in SoS$ are s-functions. The superscripts $-$ and $+$ indicate whether a function is evaluated using the first ($-$) or second ($+$) argument of $h_R : Z \times Z \rightarrow \mathbb{R}^{n_{hr}}$. That is, this constraint enforces: $\hat{v}(\hat{x}^+) - \hat{v}(\hat{x}^-) - h_R(\hat{x}^-, \hat{x}^+) \sigma_2(\hat{x}^-, \hat{x}^+) - h_S(\hat{x}^-) \sigma_3(\hat{x}^-) > 0, \forall (\hat{x}^-, \hat{x}^+) \in Z \times Z$.

SoS Constraint 3. (Viability Condition 3)

$$\begin{aligned} \mathcal{L}_{f_p}^{\hat{x}} \hat{v} + \mathcal{L}_{g_p}^{\hat{x}} \hat{v} \hat{u}_s + \sum_{j=1}^{n_z} q_j + \hat{v} \lambda + \sigma_4 h_F &\in SoS \\ q - \mathcal{L}_{\hat{e}_p}^{\hat{x}} \hat{v} + \sigma_5 h_F &\in SoS \\ q + \mathcal{L}_{\hat{e}_p}^{\hat{x}} \hat{v} + \sigma_6 h_F &\in SoS \end{aligned}$$

Here $\sigma_4 : Z \rightarrow \mathbb{R}^{1 \times n_{hf}} \in SoS$ and $\sigma_5, \sigma_6 : Z \rightarrow \mathbb{R}^{n_d \times n_{hf}}$ are s-functions that relax the constraint inside Z_p^F , and $\lambda : Z \rightarrow \mathbb{R}$ is a slack polynomial that can relax the constraint whenever $\hat{v} \neq 0$. The polynomials $q : Z \rightarrow \mathbb{R}^{n_z}$ are used to bound the effects of the dynamics error \hat{e}_p on the time derivative of \hat{v} .

SoS Constraint 4. (Viability Condition 4)

$$\begin{aligned} \hat{u}_s - \hat{u}_{min} + h_F \sigma_7 &\in SoS \\ -\hat{u}_s + \hat{u}_{max} + h_F \sigma_8 &\in SoS \end{aligned}$$

Here $\sigma_7, \sigma_8 : Z \rightarrow \mathbb{R}^{n_\alpha} \in SoS$ are s-functions that relax the constraint inside Z_p^F .

The desired objective of our optimization is to maximize the volume of \hat{V} . This volume is difficult to compute exactly for an arbitrary \hat{v} , since the domain of integration is given

by a semi-algebraic set. We propose an analytically tractable approximation to this objective:

$$\int_Z \hat{v}(\hat{x}) d\hat{x}. \quad (23)$$

This objective is combined with the following constraint in order to approximate the volume of \hat{V} :

SoS Constraint 5. (Objective Constraint)

$$1 - \hat{v} \in SoS.$$

To understand how this objective and constraint approximate the volume of \hat{V} , take a continuous function \hat{v} that satisfies the constraints of the previous section. For every point \hat{x} not in the set Z^F , the value $\hat{v}(\hat{x})$ is constrained only by Constraint (5). This means that $\hat{v}(\hat{x})$ can increase to a value of 1 for points inside \hat{V} , and $\hat{v}(\hat{x})$ increases to a value of 0 for points outside this set. As a result, \hat{v} approaches the indicator function over \hat{V} , and the integral in the objective function approaches the volume of \hat{V} .

Combining the constraints and objective, we arrive at the following sums-of-squares problem:

$$\begin{aligned} \sup_{\substack{\hat{v}, \hat{u}_s, q, \lambda \\ \sigma_1, \dots, \sigma_6}} \int_Z \hat{v}(\hat{x}) d\hat{x} \quad (24) \\ \text{s.t. SoS Constraints 1--5,} \\ \sigma_1, \dots, \sigma_8 \in SoS \end{aligned}$$

To express this problem as a semi-definite program or SDP (which can be solved with commercial solvers), all *SoS* constraints must be linear functions of the decision variable polynomials. However, Constraint 3 in the above problem includes the terms $\mathcal{L}_{g_p}^{\hat{x}} \hat{v} \hat{u}_s$ and $\lambda \hat{v}$ which are *bilinear* in \hat{u}_s, \hat{v} and in λ, \hat{v} respectively. Problems of this form are referred to as bilinear sums-of-squares problems. The bilinear nature of the constraints means that these problems are non-convex, and we can no longer guarantee a globally optimal solution to this problem.

To solve this nonconvex bilinear sums-of-squares program we turn to a strategy called alternation. This strategy breaks (24) into a pair of linear sums-of-squares programs which can each be solved using a commercial solver. In each program one of the bilinear variables is kept fixed while the other is optimized over. The variables that were optimized are then fixed while the other pair of variables are optimized. If the final solution satisfies the constraints of the original program, the solution is guaranteed to be a Viability Domain. Computationally, each SDP is formulated in *spotless*¹ and solved using *Mosek*.

C. Guaranteed Safe Semi-autonomous Controller

We use a feasible solution to the above optimization problem to generate a guaranteed safe semi-autonomous controller. This controller modifies user input to ensure that the Viability Conditions 3 and 4 are always satisfied. Condition 4 can be enforced by saturating the user inputs to

¹<https://github.com/spot-toolbox/spotless>

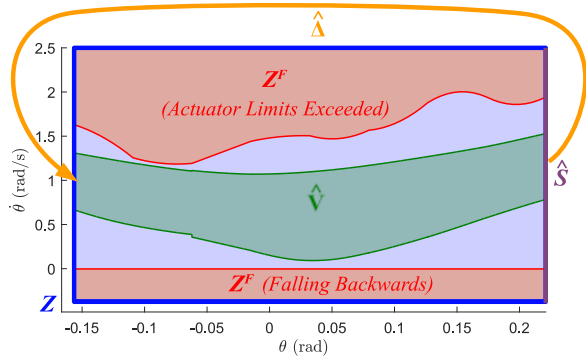


Fig. 2. A 2D slice (along $\alpha = 0.4$, $\dot{\alpha} = 0$) of the four-dimensional viability domain \hat{V} (shown in green) for Rabbit. The state flows from left to right in the figure. The border at the right corresponds to the hybrid guard \hat{S} of foot touchdown, where the state is reset under the map $\hat{\Delta}$ to the left of the figure. The unsafe set Z^F (which must be avoided to ensure safety) is shown in red. For the lower region ($\dot{\theta} < 0$) this corresponds to falling backwards, for the upper region, this conservatively approximates the region in which the control input (6) violates the torque limits of the robot.

always lie within the input bounds. To enforce condition 3, we note that it is only active on the boundary of \hat{V} . This means that we can ensure safety so long as we use the autonomous safe controller \hat{u}_s when the state lies on the boundary of \hat{V} , i.e. $\{\hat{x} \in Z | \hat{v}(\hat{x}) = 0\}$.

Since a controller that is discontinuous on the boundary of the safe set would pose difficulties for systems with finite bandwidth, we additionally must ensure that the new controller is continuous near the boundary. To achieve this, we smoothly interpolate between the user input \hat{u}_0 and the guaranteed safe controller \hat{u}_s (which satisfies the safety condition when $\hat{v}(\hat{x}) = 0$) to get the regulated input \hat{u}_r :

$$\hat{u}_r = \hat{u}_0 + (\hat{u}_s(\hat{x}) - \hat{u}_0)w_s(\hat{v}(\hat{x}), \epsilon), \quad (25)$$

where \hat{u}_s and \hat{v} are computed using (24), $w_s : \mathbb{R} \rightarrow [0, 1]$ is a smooth step-like function that satisfies $w_s(v, \epsilon) = 0$, $\forall v \geq \epsilon$, and $w_s(v, \epsilon) = 1$, $\forall v \leq \epsilon/2$, and $\epsilon \in (0, 1)$ controls the smoothness of the interpolation.

When \hat{x} satisfies $\hat{v}(\hat{x}) > \epsilon$, the user input is unmodified, as we are sufficiently removed from the boundary of the safe set. When $0 \leq \hat{v}(\hat{x}) \leq \epsilon/2$, the safe controller is fully active, keeping the state in the safe set.

V. RESULTS

We used the proposed approach to compute a control invariant set for the robot Rabbit [3]. The invariant set and the autonomous safe controller are both represented using a set of 8 degree-4 polynomials, each covering an interval within the full range of θ . A two-dimensional slice of the resulting set \hat{V} is shown in Fig. 2.

To demonstrate the semi-autonomous safe controller, we used it to ensure safety while performing a reference following task. The task is to track a time-varying pitch angle $\alpha_d : [0, \infty) \rightarrow A$. To follow the target, we set a desired pitch acceleration u_α using a "naïve" PD controller:

$$u_\alpha^d(x_\alpha, t) = k_p(\alpha_d(t) - \alpha) + k_d(\dot{\alpha}_d(t) - \dot{\alpha}) + \ddot{\alpha}_d(t). \quad (26)$$

We used the feedback controller (6) to map the desired acceleration to the four motor torques of the Rabbit model.

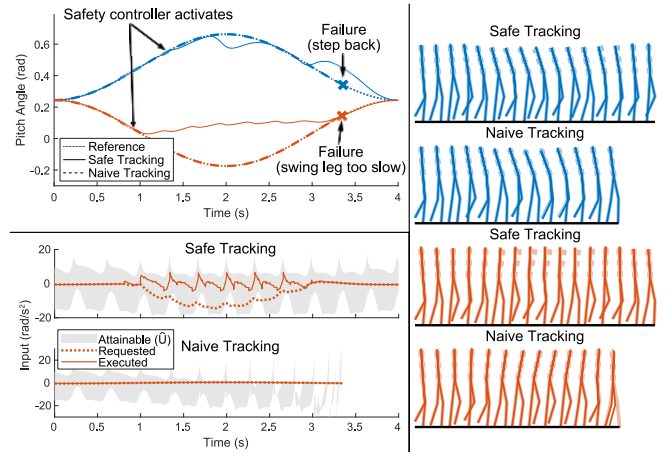


Fig. 3. Tracking performance of the safe (25) and naïve (26) controllers following two reference trajectories under the full rabbit dynamics. The pitch angles are shown in the top left. For both references, the safe controller modifies the input before safety is at risk, while the naïve controller follows the reference even as it leads to failure. Failure for the upper trajectory corresponds to stepping backwards, and in the lower trajectory corresponds to moving too fast for the swing leg to reach its target. The bottom left figure shows desired input u_α^d and executed input for both naïve and safe tracking controllers following the second reference target. The state-dependent region of inputs that satisfy the torque constraints under feedback linearization are shown in grey. Note that under the naïve controller, this region vanishes as the forward walking speed of the robot becomes too high. Stills from the simulation trajectories are shown on the right. The dotted line is the desired pitch, and the faded line is the nearest on-manifold state $q_0(\theta, \alpha)$.

For the feedback controller to respect Rabbit's actuator torque limits, we first saturated u_α with a real-time Quadratic Program (QP) to get the input to our safety regulator:

$$\begin{aligned} \hat{u}_0(x, x_\alpha, t) = \min_{u_\alpha} & |u_\alpha - u_\alpha^d(x_\alpha, t)|^2 \\ \text{s.t. } & u^*(x, x_\alpha, u_\alpha) \in [-30 \text{ Nm}, 30 \text{ Nm}]^4 \end{aligned} \quad (27)$$

Using a QP to satisfy the actuator constraints of the system is similar to many state of the art approaches for high-dimensional robot control [18], [19], [20], [21]. A major limitation of these approaches is the inability to guarantee the feasibility of the QP. That is, for some states, there may not be an input that satisfies the actuator constraints (the set of such states is shown in red in Fig. 2).

Our approach guarantees the feasibility of (27) by constraining the state of the robot to be within the QP-feasible region (i.e. outside of Z^F in Fig. 2). To maintain this state constraint, we modified the input \hat{u}_0 using the guaranteed safe semi-autonomous controller defined in (25). In Fig. 3, we compare the results of the naïve controller (26) and the safe controller (25) using a simulation of the full dynamics of the robot Rabbit. Two desired pitch angle trajectories are shown, with the robot temporarily pitching either backwards or forwards.

When tracking the backwards pitch target, the naïve controller slows to the point of falling backwards, while the safe controller deviates slightly to maintain forward walking. For the forward pitch target, the naïve controller speeds up as it leans forward. At a certain speed, it cannot longer stay on the low dimensional manifold under the torque limits and falls. The safe controller recognizes this risk early and deviates

from the desired forward pitch before reaching this speed. The bottom-left figure shows how the set of torque-limit satisfying control inputs disappears for the naïve controller.

VI. CONCLUSION

This paper presents a method to construct a guaranteed safe semi-autonomous controller for high-dimensional walking robots. The resulting controller guarantees viability and allows for flexible input when viability is not at risk. The method is evaluated on a model of the robot Rabbit, and a tracking task is used to illustrate its capabilities. With a 10-dimensional state space, this model is larger than any known model for which safety guarantees have been generated.

The core insight behind our approach is that sums-of-squares and hybrid zero dynamics are remarkably complementary tools. Sums-of-squares analysis generates the set based guarantees needed to render hybrid zero dynamics safe, and hybrid zero dynamics provides the dimensionality reduction needed for sums-of-squares analysis to be tractable. The key innovation for combining these two tools was the introduction of a set of shaping parameters which control the dynamics on the manifold. The ability to combine sums-of-squares and hybrid zero dynamics presents a promising path forward for building guaranteed safe walking controllers for complex legged robots.

REFERENCES

- [1] J. Pratt, J. Carff, S. Drakunov, and A. Goswami, "Capture point: A step toward humanoid push recovery," in *2006 6th IEEE-RAS International Conference on Humanoid Robots*, pp. 200–207, Dec 2006.
- [2] P. Wieland and F. Allgöwer, "Constructive safety using control barrier functions," *IFAC Proceedings Volumes*, vol. 40, no. 12, pp. 462–467, 2007.
- [3] C. Chevallereau, G. Abba, Y. Aoustin, F. Plestan, E. Westervelt, C. C. de Wit, and J. Grizzle, "Rabbit: A testbed for advanced control theory," *IEEE Control Systems Magazine*, vol. 23, no. 5, pp. 57–79, 2003.
- [4] P. A. Parrilo, *Structured semidefinite programs and semialgebraic geometry methods in robustness and optimization*. PhD thesis, California Institute of Technology, 2000.
- [5] A. Majumdar, R. Vasudevan, M. M. Tobenkin, and R. Tedrake, "Convex optimization of nonlinear feedback controllers via occupation measures," *The International Journal of Robotics Research*, p. 0278364914528059, 2014.
- [6] D. Henrion and M. Korda, "Convex computation of the region of attraction of polynomial control systems," *IEEE Transactions on Automatic Control*, vol. 59, no. 2, pp. 297–312, 2014.
- [7] M. Korda, D. Henrion, and C. N. Jones, "Controller design and value function approximation for nonlinear dynamical systems," *Automatica*, vol. 67, pp. 54–66, 2016.
- [8] S. Prajna and A. Jadbabaie, "Safety verification of hybrid systems using barrier certificates," in *International Workshop on Hybrid Systems: Computation and Control*, pp. 477–492, Springer, 2004.
- [9] V. Shia, R. Vasudevan, R. Bajcsy, and R. Tedrake, "Convex computation of the reachable set for controlled polynomial hybrid systems," in *53rd IEEE Conference on Decision and Control*, pp. 1499–1506, Dec 2014.
- [10] S. Mohan, V. Shia, and R. Vasudevan, "Convex computation of the reachable set for hybrid systems with parametric uncertainty," *arXiv preprint arXiv:1601.01019*, 2016.
- [11] T. Koolen, M. Posa, and R. Tedrake, "Balance control using center of mass height variation: limitations imposed by unilateral contact," in *Humanoid Robots (Humanoids), 2016 IEEE-RAS 16th International Conference on*, pp. 8–15, IEEE, 2016.
- [12] J.-P. Aubin, *Viability theory*. Springer Science & Business Media, 2009.
- [13] M. Posa, T. Koolen, and R. Tedrake, "Balancing and step recovery capturability via sums-of-squares optimization," in *2017 Robotics: Science and Systems Conference*, 2017.
- [14] P. Zhao, S. Mohan, and R. Vasudevan, "Optimal control for nonlinear hybrid systems via convex relaxations," *arXiv preprint arXiv:1702.04310*, 2017.
- [15] J. Z. Tang, A. M. Boudali, and I. R. Manchester, "Invariant funnels for underactuated dynamic walking robots: New phase variable and experimental validation," in *2017 IEEE International Conference on Robotics and Automation (ICRA)*, pp. 3497–3504, May 2017.
- [16] E. Westervelt, J. Grizzle, and D. Koditschek, "Hybrid zero dynamics of planar biped walkers," *IEEE Transactions on Automatic Control*, vol. 48, no. 1, pp. 42–56, 2003.
- [17] A. D. Ames, K. Galloway, K. Sreenath, and J. W. Grizzle, "Rapidly exponentially stabilizing control lyapunov functions and hybrid zero dynamics," *IEEE Transactions on Automatic Control*, vol. 59, no. 4, pp. 876–891, 2014.
- [18] S. C. Hsu, X. Xu, and A. D. Ames, "Control barrier function based quadratic programs with application to bipedal robotic walking," in *2015 American Control Conference (ACC)*, pp. 4542–4548, July 2015.
- [19] Q. Nguyen and K. Sreenath, "Optimal robust control for bipedal robots through control lyapunov function based quadratic programs," in *Robotics: Science and Systems*, 2015.
- [20] Q. Nguyen and K. Sreenath, "Exponential control barrier functions for enforcing high relative-degree safety-critical constraints," in *American Control Conference (ACC), 2016*, pp. 322–328, IEEE, 2016.
- [21] Q. Nguyen, A. Hereid, J. W. Grizzle, A. D. Ames, and K. Sreenath, "3d dynamic walking on stepping stones with control barrier functions," in *2016 IEEE 55th Conference on Decision and Control (CDC)*, pp. 827–834, Dec 2016.
- [22] X. Da and J. Grizzle, "Combining trajectory optimization, supervised machine learning, and model structure for mitigating the curse of dimensionality in the control of bipedal robots," *arXiv preprint arXiv:1711.02223*, 2017.
- [23] Y. Gong, R. Hartley, X. Da, A. Hereid, O. Harib, J.-K. Huang, and J. Grizzle, "Feedback control of a cassie bipedal robot: Walking, standing, and riding a segway," *arXiv preprint arXiv:1809.07279*, 2018.
- [24] K. Sreenath, H.-W. Park, I. Poulakakis, and J. W. Grizzle, "A compliant hybrid zero dynamics controller for stable, efficient and fast bipedal walking on mabel," *The International Journal of Robotics Research*, vol. 30, no. 9, pp. 1170–1193, 2011.
- [25] N. Smit-Anseeuw, R. Gleason, R. Vasudevan, and C. D. Remy, "The energetic benefit of robotic gait selection: A case study on the robot ramone," *IEEE Robotics and Automation Letters*, 2017.
- [26] S. Sastry, *Nonlinear systems: analysis, stability, and control*, vol. 10. Springer Science & Business Media, 2013.
- [27] A. Hereid and A. D. Ames, "Frost: Fast robot optimization and simulation toolkit," in *2017 IEEE/RSJ International Conference on Intelligent Robots and Systems (IROS)*, pp. 719–726, IEEE, 2017.
- [28] J. B. Lasserre, *Moments, positive polynomials and their applications*, vol. 1. World Scientific, 2009.